JMEPEG (2010) 19:70–76
DOI: 10.1007/s11665-009-9394-x
©ASM International
1059-9495/$19.00

Effect of Rolling Temperature on the Microstructures and Mechanical Properties of $Mg_{97}Zn_1Y_2$ Magnesium Alloy

Z.G. Su, R.G. Li, J. An, and Y. Lu

(Submitted July 13, 2008; in revised form February 10, 2009)

$Mg_{97}Zn_1Y_2$ magnesium alloy was hot-rolled at different temperatures from 390 to 480 °C; the effect of rolling temperature on microstructure evolution and mechanical properties of $Mg_{97}Zn_1Y_2$ magnesium alloy was investigated using x-ray diffraction (XRD), laser optical microscopy (LOP), transmission electron microscopy (TEM), and tensile test. The results showed that in the multipass process, the rolling temperature had significant effect on the microstructures and tensile properties for the hot-rolled $Mg_{97}Zn_1Y$ alloy. As the rolling temperature was increased, the original strengthening phase-$Mg_{12}YZn$ in as-cast $Mg_{97}Zn_1Y_2$ alloy experienced an evolution from dissolution to precipitation, i.e. from chain-shaped $Mg_{12}YZn$ phase together with a little lamellar structure at 420 °C to a maximum volume fraction of lamellar structure at 450 °C, and finally to a reduced volume fraction of lamellar structure at 480 °C. For $Mg_{97}Zn_1Y_2$ alloy hot-rolled in the temperature range of 390-450 °C, the tensile strength was at a high level with yielded strength of about 300 MPa and ultimate strength of about 320 MPa. The highest yielded strength was 317 MPa after hot-rolling at 450 °C; the elongation was the highest up to 5.5% after hot-rolling at 420 °C.

Keywords magnesium alloy, mechanical properties, microstructure, precipitation

1. Introduction

In recent years, the structural applications of magnesium alloys in aerospace and automobile industries are increasing progressively thanks not only to their low densities but also to their excellent properties such as electro-magnetic shielding, damping, and recycling (Ref 1-3). The commercial AZ and AM systems are less used to make important load-bearing components due to low strength and ductility; therefore, it is of great interest to develop high-performance Mg alloys to extend industrial applications. Mg-RE alloys display excellent mechanical properties at both room and elevated temperatures; especially Y is one of the most effective RE elements in improving high-temperature properties of Mg alloys (Ref 4). The Mg-Zn-Y system seems particularly promising because it exhibits a superior mechanical performance with respect to the commercial Mg-Zn-Zr (ZK) system. The Mg-Zn-Y alloys containing icosahedral phase (I-$Mg_3Zn_6Y_1$) have been paid much attention due to the remarkable strengthening effect of I phase at room temperature as well as elevated temperature (Ref 5-7). Many aspects including Zn/Y ratio, precipitates, and grain refinement in Mg-Zn-Y alloys have been investigated (Ref 8-10). In contrast to this, less works have been done on the long period stacking order (LPSO) structure Z phase ($Mg_{12}ZnY$) strengthening Mg-Zn-Y alloys, and most of them focused on the formation process of LPSO phase, dislocation structure, and variation of long period stacking order structure in rapidly solidified $Mg_{97}Zn_1Y_2$ alloy, since very recently a superior performance of rapidly solidified (RS) powder metallurgy $Mg_{97}Zn_1Y_2$ (at.%) alloy with extremely high tensile yield strength of 610 MPa and elongation of 5% has been developed and a yield strength more than 380 MPa at 200 °C (Ref 11-15). These excellent mechanical properties were archived by warm extrusion of gas-atomized $Mg_{97}Zn_1Y_2$ powders and were considered to be due to the hcp (2H)-Mg fine grain matrix of 100-200 nm in diameter with LPSO phase and the homogeneously dispersed $M_{24}Y_5$ fine particles of less than 10 nm in diameter. And it has been confirmed that the LPSO phase can be prepared by conventional casting method, the LPSO structure consists of 18 stacking sequence of ABABABCACACABCBCBC (Ref 13). The high strength at room temperature and elevated temperature in the fine-grained $Mg_{97}Zn_1Y_2$ alloy is encouraging for acquirement of high-strength Mg alloys by severe plastic deformation technique, for example, equal channel angular pressing (ECAP) in conventional $Mg_{97}Zn_1Y_2$ alloy cast ingot (Ref 16). A rather large body of research has been published on efficacy of techniques such as equal channel angular pressing (ECAP), high-pressure torsion (HPT), and severe rolling (SR) for grain refinement of a number of metallic materials (Ref 17-20). Compared with RS P/M or ECAP, SR, in particular, has potential to be adopted by industry to produce large sheets, due to its feasibility as a continuous process.

The present paper aims to explore the possibility of applying successfully the severe hot-rolling technique for improvement in mechanical properties of $Mg_{97}Zn_1Y_2$ alloy, as well as to investigate microstructure evolution with rolling temperature during processing.

Z.G. Su, R.G. Li, J. An, and **Y. Lu**, Department of Materials Science and Engineering, Key Laboratory of Automobile Materials, Ministry of Education, Nanling Campus of Jilin University, Changchun 130025, People's Republic of China. Contact e-mail: anjian@jlu.edu.cn.

2. Experimental

A testing alloy for this study was a $Mg_{97}Zn_1Y_2$ (in at.%) alloy. The alloy was prepared by conventional casting method from high-purity 99.9 wt.% Mg, 99.9 wt.% Zn, and Mg-21.5wt.%Y alloy under a shielding gas of CO_2-0.05% SF_6. Zn and Y elements were added to the melt at the temperature of 750 °C, after about 5 min manual stirring to facilitate uniform distribution of Zn and Y elements, the melt was heated to 775 °C and kept for 15 min, then was poured into an steel die preheated at 100 °C to yield a rectangular ingot of 200 mm in length, 100 mm in width, and 20 mm in height.

Thermal transformation of the as-cast $Mg_{97}Zn_1Y_2$ alloy was examined by means of differential thermal analysis (DTA: Perkin-Elmer DTA 1700 instrument) as shown in Fig. 1. During continuously heating $Mg_{97}Zn_1Y_2$ alloy in DTA, endothermic peak appears with an onset temperature of 543 °C, corresponding to complete dissolution of the precipitate phase, i.e. Z-Mg_{12}YZn phase, endothermic peak appears with an onset temperature of 614 °C, corresponding to melting of the α-Mg phase. No evident thermal transformation was found in the range of 360-500 °C, so the rolling temperature was chosen in this temperature range.

Specimens to be hot-rolled with a dimension of $90 \times 18 \times 6.5$ mm^3 were machined from the cast ingot and were heated at 390, 420, 450, and 480 °C, respectively, for 20 min prior to each pass rolling. The rolling was employed with a reduction of ~15% per pass. The final thickness of hot-rolled specimens was 1.3 mm (reduction ~80%) after 9 passes of rolling.

Mechanical properties of the $Mg_{97}Zn_1Y_2$ alloy after severe hot-rolling were evaluated by tensile tests at room temperature at an initial strain rate of 1.0×10^{-3} s^{-1}. Tensile samples were machined from hot-rolled sheet with a cross-section of 4.0×1.3 mm, a gauge length of 15 mm. The strain rate was kept constant during the test and the tensile direction was parallel to the rolling direction.

The microstructures of hot-rolled and as-cast $Mg_{97}Zn_1Y_2$ alloys were observed using a laser optical microscope after polishing and etching in 0.5% HF solution. The crystalline phases in $Mg_{97}Zn_1Y_2$ alloys were characterized by a Rigaku x-ray diffractometer (XRD). The fracture characteristics of the fracture surface were examined with a JEOL 8600 scanning electron microscope.

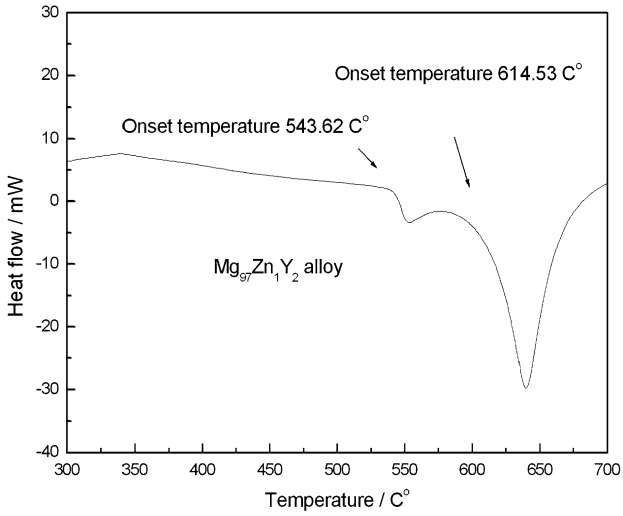

Fig. 1 DTA thermograms for as-cast $Mg_{97}Zn_1Y_2$ alloy

3. Results and Discussion

3.1 Microstructure Evolution by Hot-Rolling

Figure 2 shows the microstructure of as-cast $Mg_{97}Zn_1Y_2$ alloy; it can be seen that the microstructure consists of primary α-Mg grains with the grain boundaries decorated by continuous secondary phase network. Coarse α-Mg grains with about 30-80 μm in diameter and secondary phase with about 2.3-6.9 μm in thickness at grain boundaries are observed. The XRD analysis shown in Fig. 3 indicates that the second phase was a Z-Mg_{12}ZnY intermetallic compound. After hot-rolling at different temperatures, the constituent phases in hot-rolled $Mg_{97}Zn_1Y_2$ alloy were essentially the same as the as-cast alloy (see Fig. 3), but the microstructures along the rolling direction changed dramatically as shown in Fig. 4. After being rolled at

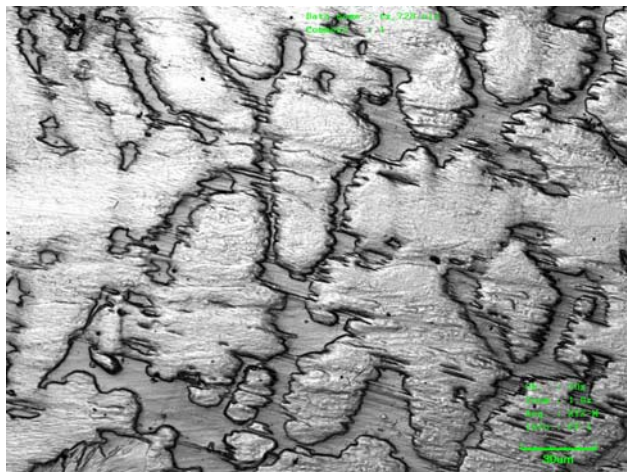

Fig. 2 Microstructure of as-cast $Mg_{97}Zn_1Y_2$ alloy

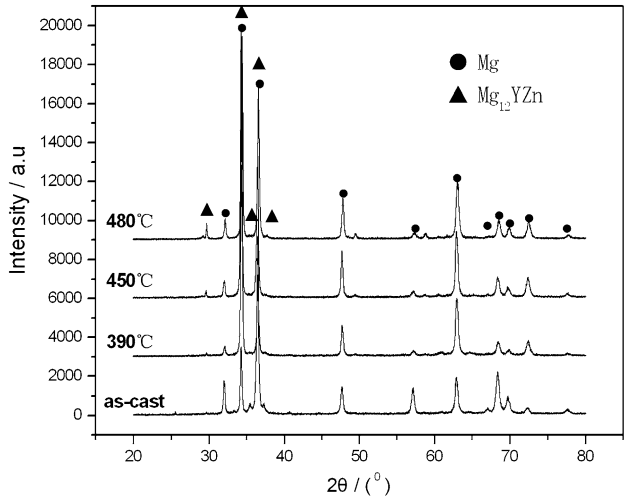

Fig. 3 The x-ray diffraction patterns of as-cast and hot-rolled $Mg_{97}Zn_1Y_2$ alloys

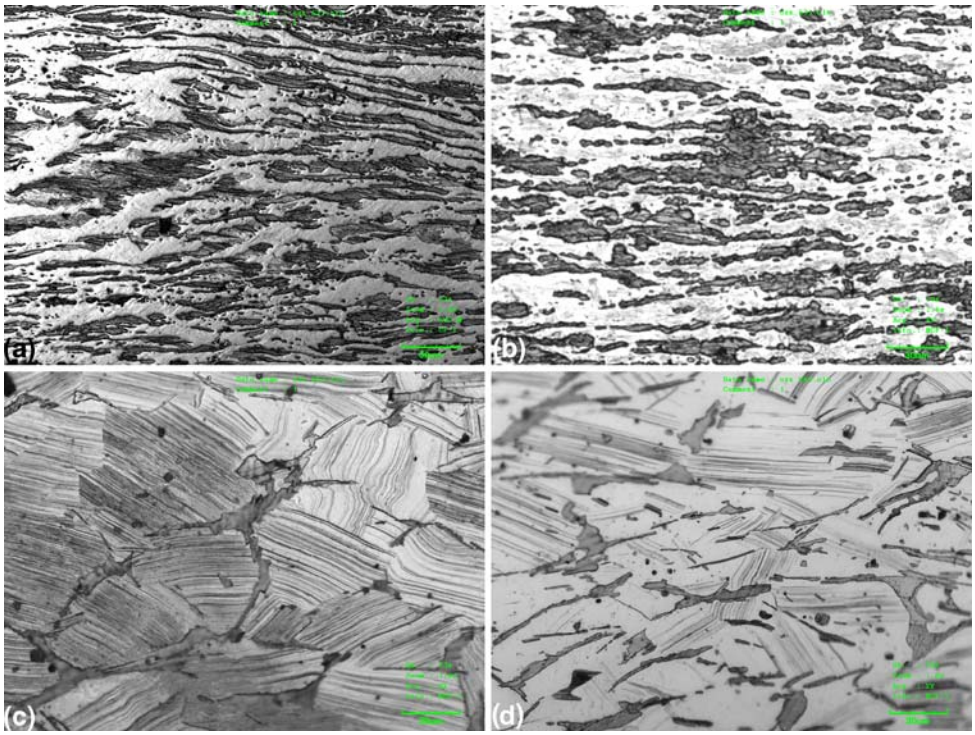

Fig. 4 Longitudinal microstructures of hot-rolled $Mg_{97}Zn_1Y_2$ alloy at (a) 390 °C, (b) 420 °C, (c) 450 °C, and (d) 480 °C

390 and 420 °C respectively, the α-Mg grains were elongated along the rolling direction but unrecrystallized, and the Z-$Mg_{12}ZnY$ phase was destroyed and broken into zonal distribution along the rolling direction. In 420 °C rolled alloy, the Z-$Mg_{12}ZnY$ phase decreased in both volume fraction and size due to gradual dissolution during later heating and finally took a from of chain along the rolling direction. Meanwhile, a little volume of lamellar structures was formed in α-Mg matrix. The lamellar structure was reported to be composed of alternating layers of LPSO phase and 2H-Mg phase (Ref 21). As the rolling temperature was increased to a temperature range of 450-480 °C, the equiaxed α-Mg grains were formed by recrystallization and the second phase network precipitated again at the grain boundary of the recrystallized α-Mg grains. In addition to this, a large area of lamellar structures occurred within the α-Mg grains. In the 450 °C hot-rolled alloy, the original α-Mg grains were entirely replaced by lamellar structures while the lamellar structures were found to be less in the 480 °C hot-rolled alloy and were embedded in white α-Mg matrix.

A TEM micrograph for typical lamellar structure is shown in Fig. 5. According to Ref 20-22, the alternative dark laminas were an LPSO phase, and the EDS analysis revealed that the Zn and Y elements were poor in Mg matrix but rich in the LPSO phase.

In order to explain the effect of rolling temperature on the microstructure evolution, cross-sectional microstructures were also compared with the above longitudinal ones as shown in Fig. 6. It can be noted that the microstructures showed evident characteristics of deformation after rolling at 390 and 420 °C while the transverse microstructures rolled at 450 and 480 °C were similar to those along the rolling direction, α-Mg matrix took the form of coarse equiaxed grains, and the feature of less lamellar structure embedded in α-Mg matrix was more

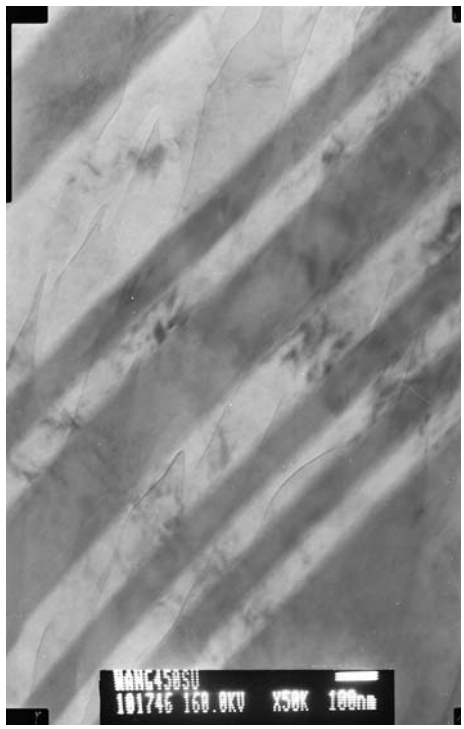

Fig. 5 TEM typical morphology of LPSO precipitates in $Mg_{97}Y_2Zn$ alloy hot-rolled at 450 °C

pronounced for sample rolled at 480 °C. Based on the above microstructure evolution observation, the mechanisms of formation and distribution of lamellar structure in $Mg_{97}Zn_1Y_2$ alloy can be proposed as follows: during the first several rolling passes, the fragile $Mg_{12}YZn$ phase cracked and broke into

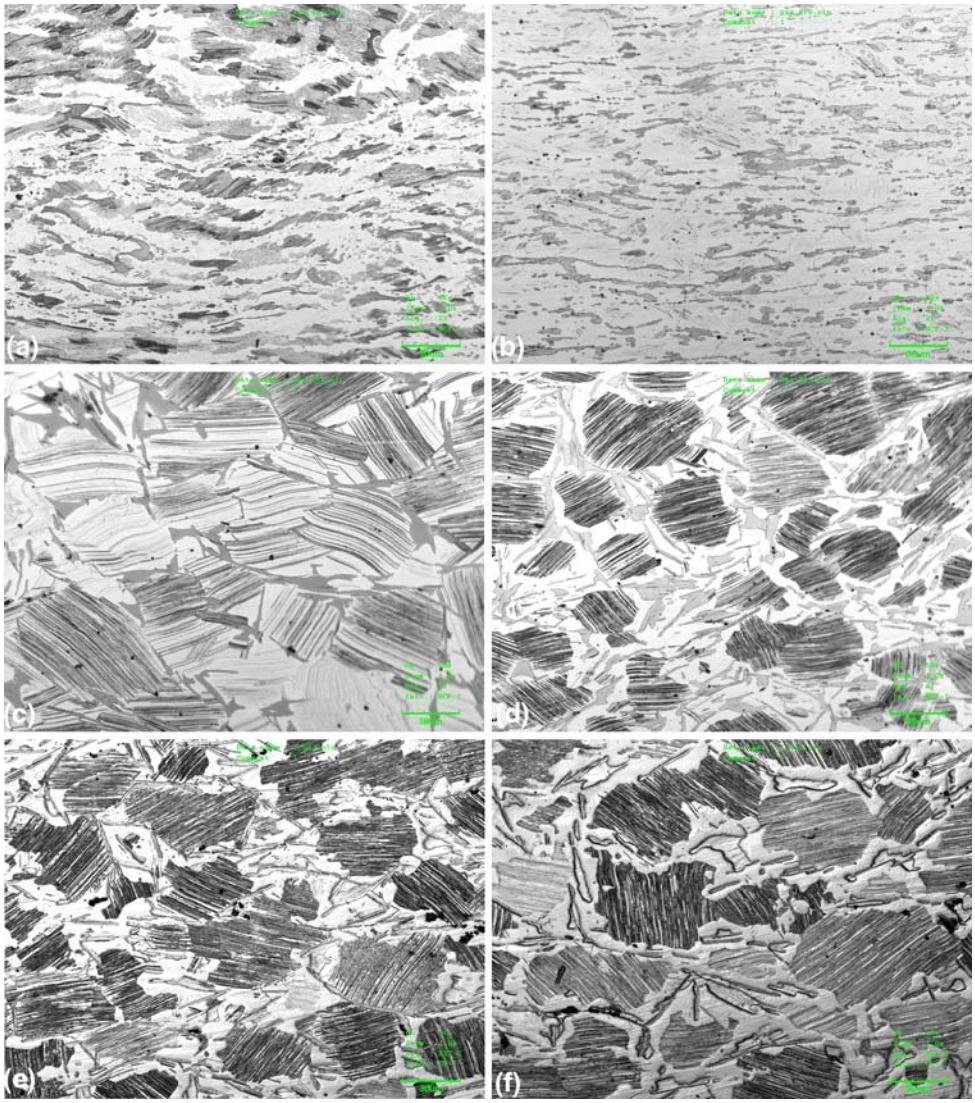

Fig. 6 Cross-sectional microstructures of $Mg_{97}Zn_1Y_2$ alloy hot-rolled at (a) 390 °C, (b) 420 °C, (c) 450 °C, (d) 480 °C, (e) solution treated and annealed at 480 °C for 4 h, and (f) solution treated and annealed at 480 °C for 6 h

strips and particles, and the $Mg_{12}YZn$ phase partly dissolved into α-Mg solid solution gradually, despite the complete dissolution temperature being as high as 543 °C, during the later heating period. By increasing the rolling temperature, the $Mg_{12}YZn$ phase dissolved more and faster; therefore, the compositions of Zn and Y elements in α-Mg solid solution were increased much more pronouncedly until their solubilities were reached. Afterwards, the lamellar structure of $Mg_{12}YZn$ began to form within the α-Mg grains. At low rolling temperatures such as 390 and 420 °C, the lamellar structure was formed rather less due to low dissolution of $Mg_{12}YZn$ phase (see Fig. 6a, b). In the case of 450 °C rolling, the $Mg_{12}YZn$ phase began to precipitate substantially within the α-Mg solid solution and on the boundaries in the form of lamellar structure (Fig. 6c) and secondary phase network. And after the lamellar structure was formed, during the next heating period, lamellar $Mg_{12}YZn$ phase can also partly redissolve into the α-Mg solid solution; therefore, the formation of lamellar structure is a process of precipitation and dissolution of LPSO phase. At the highest heating temperature 480 °C, the lamellar $Mg_{12}YZn$ phase near the boundary area dissolved so quickly that the dissolving morphology was preserved to the room temperature, leading to a morphology feature of lamellar structure embedded in the α-Mg matrix with an empty space between the lamellar structure and the secondary phase network (see Fig. 6d). In order to confirm the dissolution of lamellar $Mg_{12}YZn$ phase during heating process, the sample rolled at 480 °C was reheated to 480 °C and held for different time followed by water quenching, the change in microstructure during heating can be preserved to the room temperature. It can bee seen from Fig. 6(e) and (f) that the original lamellar structure with regular edge becomes irregularly concavo-convex due to preferential dissolution in edge area, resulting in a decrease of lamellar structure and widening of white area surrounding lamellar structure.

3.2 Effect of Hot-Rolled Microstructure on the Tensile Properties

The tensile test curves for hot-rolled $Mg_{97}Zn_1Y_2$ alloys are illustrated in Fig. 7; for comparison the as-cast alloy is also

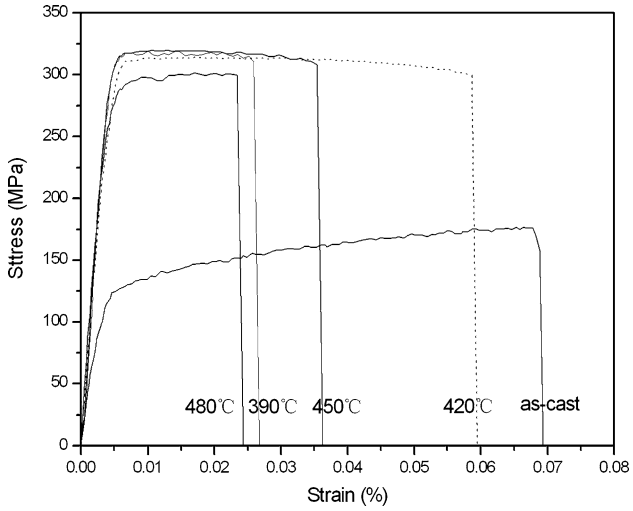

Fig. 7 Stress-strain curves of tensile tests for hot-rolled and as-cast $Mg_{97}Zn_1Y_2$ alloys

listed in the figure. The mechanical properties of hot-rolled alloys were much higher than that of as-cast one except the elongation. The yield strength, ultimate tensile strength, and elongation for as-cast alloy were 120 MPa, 170 MPa, and 6.1%, respectively, while the yield strength and ultimate tensile strength for hot-rolled alloys were in the range of 310-317 MPa and 318-325 MPa, respectively. It dose not differentiate much in tensile strength for the alloys rolled at 390, 420, and 450 °C. The alloy hot-rolled at 450 °C was highest with a yield strength of 317 MPa and an ultimate tensile strength of 325 MPa. The elongation of alloy hot-rolled at 420 °C was the highest up to 5.5%, followed by 3.1% at 450 °C and 2.1% at 390 °C. The tensile properties of alloy hot-rolled at 480 °C were the worst with yield strength of 270 MPa, ultimate tensile strength of 307 MPa, and elongation of 1.9%.

It is known from microstructure evolution mentioned above that the changes that happened to the α-Mg matrix are mainly refinement of uncrystallized grain by rolling deformation at low temperatures (390 and 420 °C) and coarsening of crystallized grain at high temperatures (450 and 480 °C). Generally, the relationship between the yield strength and grain size follows the Hall-Petch equation (Ref 22, 23):

$$\sigma_y = \sigma_0 + kd^{-1/2} \quad \text{(Eq 1)}$$

where d is a measure of the grain diameter and σ_0 and k are experimentally derived constants. According to the equation, refinement of work hardening grain will cause increase in the yield strength; conversely, coarsening of crystallized grain can deteriorate the yield strength. However, the hot-rolled alloys did not obey the equation strictly, for example, the alloy hot-rolled at 450 °C possessed coarse grain but the highest yield strength. The great difference in microstructures between the alloys hot-rolled at 420 and 450 °C was whether the lamellar structure was present. This means that the intermetallic compound in alloy has a great effect on the tensile properties. $Mg_{12}YZn$ compound as the strengthening phase experienced remarkable changes in volume fraction, distribution, and morphology with the rolling temperature. As the rolling temperature was increased, the volume fraction of $Mg_{12}YZn$ phase decreases owing to dissolution into α-Mg solid solution. At low rolling temperature (390 and 420 °C), most the $Mg_{12}YZn$ phase has the morphology of strip and chain made of broken particle despite a little volume of lamellar structure occurred in the rolled alloy at 420 °C. At high rolling temperature (450 and 480 °C), a large volume of lamellar structure was formed besides a little volume of discontinuous $Mg_{12}YZn$ phase network.

Table 1 Microhardness in different regions for the as-cast and hot-rolled $Mg_{97}Zn_1Y_2$ alloys

Alloy	Region	Hardness, HV
As-cast $Mg_{97}Zn_1Y_2$	$Mg_{12}YZn$ phase	108.6
	α-Mg grain	70.5
Hot-rolled $Mg_{97}Zn_1Y_2$	Lamellar structure	92.9
	α-Mg matrix surrounding lamellar structure	78.3

Referring to the mechanical characteristics of pearlite consisting of alternating layers of ferrite and Fe_3C in steel which has high yield strength compared with ferrite and spheroidite consisting of sphere-like particles of Fe_3C embedded in a continuous ferrite matrix, it can be deduced that the lamellar structure has the best strengthening effect on the tensile strength. To confirm this conclusion, microhardness in different regions in the microstructures mentioned above was tested with a load of 0.5 N and are listed in Table 1. It can be noted that the microhardness for lamellar structure, α-Mg solid solution in as-cast alloy and α-Mg solid solutions surrounding lamellar structure were 92.9, 70.5, and 78.3 HV, respectively. According to a simple relation for metals suggested by Tabor (Ref 24):

$$H = CY \quad \text{(Eq 2)}$$

where H is hardness, Y is yield strength, and C is a constant; it is deduced that the lamellar structure has the highest yield strength. The microstructure of the alloy hot-rolled at 450 °C mainly comprised lamellar structure, thus it exhibited the highest yield strength, whereas the lamellar structure in the alloy hot-rolled at 480 °C was less and embedded in the coarse α-Mg grain with an empty space between the lamellar structure and the secondary phase network, leading to low strengthening effect and the lowest yield strength out of the hot-rolled alloys. The tensile strengths for the alloys hot-rolled at 390 and 420 °C were intermediate between the hot-rolled alloys at 450 and 480 °C. The ductility of the hot-rolled alloys was influenced by the grain size of α-Mg matrix, morphology and distribution of $Mg_{12}YZn$ phase. The deformability for α-Mg grain is better than lamellar structure, so the elongation was reduced when lamellar structure was formed in the hot-rolled alloy. Fine $Mg_{12}YZn$ particles homogeneously distributed in α-Mg matrix made the elongation of the alloy hot-rolled at 420 °C the best. The microstructure of the alloy hot-rolled at 450 °C mainly consists of lamellar structure and second phase network, leading to a decrease in elongation. The lowest elongation falls on the alloy hot-rolled at 480 °C owing to the coarse grain of α-Mg matrix with some volume of lamellar structure embedded in it and second phase network. In the hot-rolled alloy at 390 °C, the broken $Mg_{12}YZn$ block was so big and distributed along the boundary of α-Mg grains that the elongation for this alloy was not high.

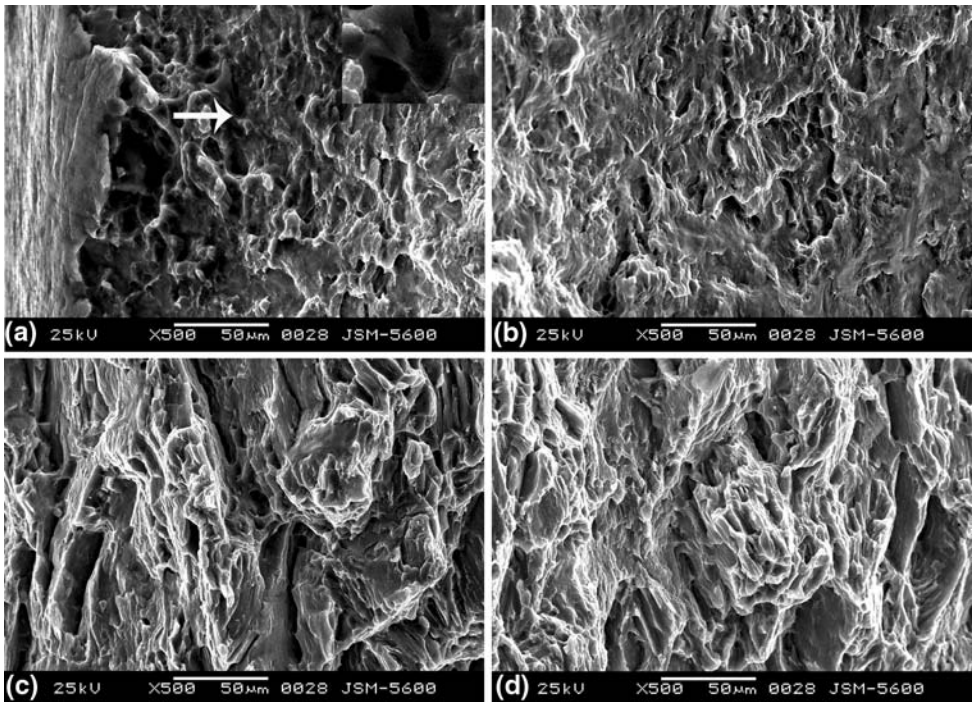

Fig. 8 SEM fractographs of the specimens rolled at (a) 390 °C, (b) 420 °C, (c) 450 °C, and (d) 480 °C

3.3 Fracture Analysis

Figure 8 shows a set of SEM fractographs of tensile specimens rolled at different temperatures. Tensile fracture surfaces were all vertical to the rolling direction. Figure 8(a) and (b) shows the SEM fractographs of alloys rolled at temperatures of 390 and 420 °C, which showed a kind of tearing fracture in which there were many small dimples and some tearing ridges to be formed. However, It can be found that a few of the cracks are formed in the matrix surrounding the big $Mg_{12}YZn$ particle for the alloy rolled at 390 °C as indicated by the arrows, which may be one of the reasons that it demonstrates lower elongation than the alloy rolled at 420 °C. Figure 8(c) and (d) shows the SEM fractographs of alloys rolled at temperatures of 450 and 480 °C; they display decohesion at the grain boundary second phase network and tearing fracture, and the decohesion deteriorates the elongation.

4. Conclusions

1. By increasing the rolling temperature, the network of $Mg_{12}YZn$ phase in $Mg_{97}Zn_1Y_2$ alloy was broken into chains of particles along the rolling direction, and a little of laminar $Mg_{12}YZn$ began to precipitate in α-Mg matrix at the rolling temperature of 420 °C, the laminar structure reached a maximum at 450 °C and decreased at 480 °C.
2. The lamellar structure comprising alternative $Mg_{12}YZn$ phase and α-Mg matrix showed significant strengthening effect on the $Mg_{97}Zn_1Y_2$ alloy.
3. Hot-rolled $Mg_{97}Zn_1Y_2$ alloys have good tensile properties with yield strength of ~310 MPa and ultimate tensile strength of ~320 MPa. The elongation of the alloy hot-rolled at 420 °C was the highest up to 5.5%.

Acknowledgments

The authors thank the Project 985-automotive engineering of Jilin University and the Science and Technology Supporting Project of Changchun City (2007KZ05).

References

1. S. Lee, Y.H. Chen, and J.Y. Wang, Isothermal Sheet Formability of Magnesium Alloy AZ31 and AZ61, *J. Mater. Process. Technol.*, 2002, **124**, p 19–24
2. H. Takuda, T. Enami, and K. Kubata, The Formability of a Thin Sheet of Mg-8.5Li-1Zn Alloy, *J. Mater. Process. Technol.*, 2000, **101**, p 281–286
3. H. Takuda, T. Yshii, and N. Hatta, Finite-Element Analysis of the Formability of a Magnesium-Based Alloy AZ31 Sheet, *J. Mater. Process. Technol.*, 1999, **90**, p 135–140
4. M. Suzuki, T. Kimura, J. Koike, and K. Maruyama, Strengthening Effect of Zn in Heat Resistant Mg-Y-Zn Solid Solution Alloys, *Scr. Mater.*, 2003, **48**, p 997–1002
5. A. Singh, M. Watanabe, A. Kato, and A.P. Tsai, Microstructure and Strength of Quasicrystal Containing Extruded Mg-Zn-Y Alloys for Elevated Temperature Application, *Mater. Sci. Eng. A*, 2004, **385**, p 382–396
6. A. Singh, M. Nakamura, M. Watanabe, A. Kato, and A.P. Tsai, Quasicrystal Strengthened Mg-Zn-Y Alloys by Extrusion, *Scr. Mater.*, 2003, **49**, p 417–422
7. D.H. Bae, S.H. Kim, W.T. Kim, and D.H. Kim, High Strength Mg-Zn-Y Alloy Containing Quasicrystalline Particles, *Mater. Trans.*, 2001, **42**, p 2144–2147
8. D.K. Xu, L. Liu, Y.B. Xu, and E.H. Han, The Influence of Element Y on the Mechanical Properties of the As-Extruded Mg-Zn-Y-Zr Alloys, *J. Alloys Compd.*, 2006, **426**, p 155–161
9. I.J. Kim, D.H. Bae, and D.H. Kim, Precipitates in a Mg-Zn-Y Alloy Reinforced by an Icosahedral Quasicrystalline Phase, *Mater. Sci. Eng. A*, 2003, **359**, p 313–318
10. A. Muller, G. Garces, P. Perez, and P. Adeva, Grain Refinement of Mg-Zn-Y Alloy Reinforced by an Icosahedral Quasicrystalline Phase by Severe Hot Rolling, *J. Alloys Compd.*, 2007, **443**, p L1–L5
11. M. Nishida, Y. Kawamra, and T. Yamamuro, Formation Process of Unique Microstructure in Rapidly Solidified Mg97Zn1Y2 Alloy, *Mater. Sci. Eng. A*, 2004, **375**, p 1217–1223

12. M. Matsuda, S. Ando, and M. Nishida, Dislocation Structure in Rapidly Solidified Mg97Zn1Y2 Alloy with Long Period Stacking Order Phase, *Mater. Trans.*, 2005, **46**, p 361–364
13. M. Matsuda, S. Ii, Y. Kawamura, Y. Ikuhara, and M. Nishida, Variation of Long-Period Stacking Order Structures in Rapidly Solidified $Mg_{97}Zn_1Y_2$ Alloy, *Mater. Sci. Eng. A*, 2005, **393**, p 269–274
14. T. Itoi, T. Seimiya, Y. Kawamura, and M. Hirohashi, Long Period Stacking Structures Observed in $Mg_{97}Zn_1Y_2$ Alloy, *Scr. Mater.*, 2004, **51**, p 107–111
15. Y. Kawamura, K. Hayashi, A. Inoue, and T. Masumoto, Rapidly Solidified Powder Metallurgy Mg(97)Zn(1)Y(2) Alloys with Excellent Tensile Yield Strength Above 600 MPa, *Mater. Trans. JIM*, 2001, **42**, p 1172–1176
16. H. Watanabe, H. Somekawa, and K. Higashi, Fine-Grain Processing by Equal Channel Angular Extrusion of Rapidly Quenched Bulk Mg-Y-Zn Alloy, *J. Mater. Res.*, 2005, **20**, p 93–101
17. A. Yamashita, Z. Horita, and T.G. Langdon, Improving the Mechanical Properties of Magnesium and a Magnesium Alloy Through Severe Plastic Deformation, *Mater. Sci. Eng. A*, 2001, **300**, p 142–147
18. Y. Iwahashi, Z. Horita, M. Nemoto, and T.G. Langdon, The Process of Grain Refinement in Equal-Channel Angular Pressing, *Acta Mater.*, 1998, **46**, p 3317–3331
19. W.J. Kim, S.W. Chung, and D. Kum, Superplasticity in Thin Magnesium Alloy Sheets and Deformation Mechanism Maps for Magnesium Alloys at Elevated Temperatures, *Acta Mater.*, 2001, **49**, p 3337–3345
20. M.T. Perz-Prado, J.A. Del Valle, and O.A. Ruano, Achieving High Strength in Commercial Mg Cast Alloys Through Large Strain Rolling, *Mater. Lett.*, 2005, **59**, p 3299–3303
21. Y. Kawamura, T. Kasahara, S. Izumi, and M. Yamasaki, Elevated Temperature $Mg_{97}Y_2Cu_1$ Alloy with Long Period Ordered Structure, *Scr. Mater.*, 2006, **55**, p 453–456
22. E.O. Hall, The Deformation and Ageing of Mild Steel: III Discussion of Results, *Proc. Phys. Soc. B*, 1951, **64**, p 747–753
23. N.J. Petch, The Cleavage Strength of Polycrystal, *J. Iron Steel Inst.*, 1953, **174**, p 25–28
24. D. Tabor, A Simple Theory of Static and Dynamic Hardness, *Proc. R. Soc. Lond. A*, 1948, **192**, p 247–274